ELSEVIER

Inorganica Chimica Acta 226 (1994) 91–98

Inorganica Chimica Acta

Valence tautomerism for catechol/semiquinone complexes of the *trans*-M(Bupy)$_2$(3,6-DBQ)$_2$ (M = Mn, Fe, Co) series

Attia S. Attia, Ok-Sang Jung, Cortlandt G. Pierpont *

Department of Chemistry and Biochemistry, University of Colorado, Boulder, CO 80309, USA

Received 24 March 1994

Abstract

Studies directed at the investigation of metal–quinone electron transfer have been carried out for members of the M(Bupy)$_2$(3,6-DBQ)$_2$ series where Bupy is 4-tert-butylpyridine, 3,6-DBQ is the 3,6-di-tert-butylbenzoquinone ligand in either its reduced semiquinonate or catecholate form, and M is Mn, Fe or Co. Structural characterization on Mn(Bupy)$_2$(3,6-DBCat)$_2$ and Fe(Bupy)$_2$(3,6-DBSQ)(3,6-DBCat) (Mn(Bupy)$_2$(3,6-DBCat)$_2$: triclinic, $P\bar{1}$, $a = 10.294(15)$, $b = 10.632(8)$, $c = 11.085(5)$ Å, $\alpha = 93.00(3)$, $\beta = 90.78(3)$, $\gamma = 112.12(3)°$, $V = 1122(1)$ Å^3 and $Z = 1$; Fe(Bupy)$_2$(3,6-DBSQ)(3,6-DBCat): triclinic, $P\bar{1}$, $a = 10.326(2)$, $b = 10.646(2)$, $c = 11.192(2)$ Å, $\alpha = 92.40(2)$, $\beta = 92.17(1)$, $\gamma = 111.87(1)°$, $V = 1138.9(4)$ Å^3 and $Z = 1$) has shown that the molecules are in the *trans* isomeric form. Features of the inner coordination spheres about both metal ions are in accord with the charge distributions indicated. Crystallographically imposed inversion symmetry disorders the Cat and SQ ligands of the iron complex. Both Co(Bupy)$_2$(3,6-DBSQ)(3,6-DBCat) and Mn(Bupy)$_2$(3,6-DBSQ)(3,6-DBCat) show low-energy charge transfer transitions in the region between 3000 and 5000 cm^{-1}, and exhibit valence tautomeric equilibria in solution and in the solid state. Equilibria for the cobalt complex involve shifts between Co^{III}(Bupy)$_2$(3,6-DBSQ)(3,6-DBCat) and Co^{II}(Bupy)$_2$(3,6-DBSQ)$_2$ charge distributions in separate electron transfer and metal spin transition steps. Solid state equilibria for the manganese complex appear to occur between Mn^{III}(Bupy)$_2$(3,6-DBSQ)(3,6-DBCat) and Mn^{IV}(Bupy)$_2$(3,6-DBCat)$_2$ charge distributions, with an additional shift to the Mn^{II}(Bupy)$_2$(3,6-DBSQ)$_2$ form in toluene solution. Fe(Bupy)$_2$(3,6-DBSQ)(3,6-DBCat) shows a low intensity transition at 2150 nm, but fails to show evidence for a tautomeric equilibrium.

Keywords: Crystal structures; Valence tautomerism; Manganese complexes; Iron complexes; Cobalt complexes; Catechol complexes; Semiquinone complexes

1. Introduction

Transition metal complexes containing quinone ligands often show unique electronic and magnetic properties that result from the similarity in orbital energy between the metal d levels and the quinone π molecular orbitals [1]. The electronic structures of these complexes are generally localized with a discrete charge distribution that is consistent with the assignment of formal charge to the metal ion and the redox-active quinone ligands. In systems where thermodynamic and electronic effects are favorable, equilibria between valence tautomers, differing in charge distribution between ligand and metal, may be observed in solution and in the solid state. In effect, these systems show thermally induced metal–ligand electron transfer properties under equilibrium conditions. In the present paper we describe the results of studies on bis(quinone) complexes of Mn, Fe and Co, that contain pyridine ligands bonded to the metal to give complex molecules as the *trans* isomers. The pyridine ligand used in this investigation is 4-tert-butylpyridine (Bupy) and the quinone ligands used are derived from 3,6-di-tert-butyl-1,2-benzoquinone (3,6-DBBQ). With these compounds we can investigate electron transfer and tautomeric equilibria for an isostructural series of complexes differing only in metal ion.

2. Experimental

2.1. Materials

3,6-Di-tert-butyl-1,2-benzoquinone (3,6-DBBQ) and Fe(3,6-DBSQ)$_3$ were prepared by literature proce-

* Corresponding author.

SSDI 0020-1693(94)04074-6

dures [2]. Dimanganese decacarbonyl and dicobalt octacarbonyl were purchased from Strem Chemical Co., and 4-tert-butylpyridine (Bupy) was purchased from Aldrich.

2.2. Complex syntheses

2.2.1. $Mn(Bupy)_2(3,6\text{-}DBQ)_2$

A solution of $Mn_2(CO)_{10}$ (0.08 g, 0.18 mmol) in 20 ml of hexane was added to 3,6-DBBQ (0.16 g, 0.70 mmol) and Bupy (0.1 ml, 1.24 mmol) dissolved in 30 ml hexane under N_2. The mixture was photolyzed with an Hg lamp for 12 h, and the volume of the solution was reduced under a slow stream of dry N_2. Dark purple crystals of $Mn(Bupy)_2(3,6\text{-}DBQ)_2$ were obtained in yields greater than 80%. The complex is unstable in toluene, but could be recrystallized from a Bupy/toluene mixture.

2.2.2. $Fe(Bupy)_2(3,6\text{-}DBQ)_2$

Bupy (0.22 ml, 2.73 mmol) dissolved in 30 ml of hexane was added to $Fe(3,6\text{-}DBSQ)_3$ (0.40 g, 0.56 mmol) in 20 ml of hexane under an atmosphere of N_2. The solution turned from green to dark purple–blue over a period of 24 h. Slow evaporation of the solvent gave purple–blue crystals of $Fe(Bupy)_2(3,6\text{-}DBQ)_2$ in yields greater than 80%.

2.2.3. $Co(Bupy)_2(3,6\text{-}DBQ)_2$

$Co_2(CO)_8$ (86 mg, 0.25 mmol) and Bupy (135 mg, 0.52 mmol) were combined in 30 ml of toluene. The mixture was stirred for 5 min and 3,6-DBBQ (220 mg, 1.0 mmol) dissolved in 30 ml of toluene was added. The solution was stirred for 2 h at room temperature. Slow evaporation of the solvent produced dark blue crystals of $Co(Bupy)_2(3,6\text{-}DBQ)_2$ in 80% yield. Attempts at recrystallization of the complex from either toluene or hexane (at room temperature) led to decomposition.

Complexes of all three metals were characterized crystallographically and their purity was determined using spectroscopic techniques.

2.3. Physical measurements

Electronic spectra were recorded on a Perkin-Elmer Lambda 9 spectrophotometer equipped with a RMC-Cryosystems cryostat. Magnetic measurements were made using a Quantum Design SQUID magnetometer at a field strength of 5 kG. IR spectra were recorded on a Perkin-Elmer 1600 FTIR with samples prepared as KBr pellets. Cyclic voltammograms were obtained with a Cypress CYSY-1 computer controlled electroanalysis system. A platinum disk working electrode was used; the Ag/Ag^+ reference electrode consisted of a CH_3CN solution of $AgPF_6$ in contact with a silver wire placed in glass tubing with a Vycor frit at one end to allow ion transport. Solution concentrations were approximately 1.5×10^{-3} M in complex and 0.10 M in $(Bu_4N)(PF_6)$ supporting electrolyte. The Fc/Fc^+ couple appeared at 0.154 V (versus Ag/Ag^+) with a ΔE of 103 mV.

2.4. Crystallographic structure determinations

2.4.1. $Fe(Bupy)_2(3,6\text{-}DBSQ)(3,6\text{-}DBCat)$

Dark blue crystals of the complex were obtained from the reaction mixture. Axial photographs indicated only triclinic symmetry and the centered settings of 25 intense reflections with 2θ values between 19 and 27° gave the unit cell dimensions listed in Table 1. Data were collected by θ–2θ scans within the angular range 3.0–45°. Density measurements together with the unit cell volume indicated that there was one complex molecule per asymmetric region. The structure was solved by placing the iron atom at the origin, the locations of other atoms of the structure were obtained from the phases generated from the iron position, and the complex molecule has imposed inversion symmetry. Final cycles of refinement converged with discrepancy indices of $R=0.050$ and $R_w=0.060$. Selected atom positions are listed in Table 2; see also Section 4.

2.4.2. $Mn(Bupy)_2(3,6\text{-}DBCat)_2$

Dark purple–blue crystals of the complex were obtained from the reaction mixture. Axial photographs indicated only triclinic symmetry. Unit cell dimensions and the intensities of reflections obtained using Wycoff scans indicated that the complex was isostructural with its iron analog, *trans*-$Fe(Bupy)_2(3,6\text{-}DBSQ)(3,6$-

Table 1
Crystallographic data[a] for $Fe(Bupy)_2(3,6\text{-}DBSQ)(3,6\text{-}DBCat)$ and $Mn(Bupy)_2(3,6\text{-}DBCat)_2$

	$Fe(Bupy)_2(3,6\text{-}DBSQ)$-$(3,6\text{-}DBCat)$	$Mn(Bupy)_2$-$(3,6\text{-}DBCat)_2$
Molecular weight	766.9	765.9
Color	violet	purple
Crystal system	triclinic	triclinic
Space group	$P\bar{1}$	$P\bar{1}$
a (Å)	10.326(2)	10.294(15)
b (Å)	10.646(2)	10.632(8)
c (Å)	11.192(2)	11.085(5)
α (°)	92.40(2)	93.00(3)
β (°)	92.17(1)	90.78(3)
γ (°)	111.87(1)	112.12(3)
V (Å^3)	1138.9(4)	1122(1)
Z	1	1
D_{calc} (g cm^{-3})	1.118	1.134
D_{meas} (g cm^{-3})	1.12	1.13
μ (mm^{-1})	0.368	0.321
R, R_w	0.050, 0.060	0.078, 0.090
GOF	1.21	1.41

[a]Radiation: Mo Kα (0.71073 Å); temperature: 293–298 K.

Table 2
Atom coordinates ($\times 10^4$) and equivalent isotropic displacement parameters[a] (Å^2) for Fe(Bupy)$_2$(3,6-DBSQ)(3,6-DBCat)$_2$

	x/a	y/b	z/c	U_{eq}
Fe	0	0	0	47(1)
O1	9612(4)	1470(4)	854(4)	46(2)
O2	11100(4)	100(4)	1501(4)	48(2)
C1	10131(6)	1712(6)	1968(6)	40(3)
C2	10984(6)	954(6)	2323(7)	39(3)
C3	11608(7)	1139(7)	3487(7)	49(3)
C4	11401(7)	2088(8)	4236(6)	59(4)
C5	10572(8)	2816(7)	3889(7)	59(4)
C6	9899(7)	2641(6)	2788(7)	47(3)
C7	12499(7)	316(7)	3873(7)	60(4)
C8	12902(10)	558(9)	5220(7)	112(6)
C9	11655(8)	−1201(7)	3660(7)	79(4)
C10	13801(8)	717(9)	3183(8)	99(5)
C11	8926(8)	3370(8)	2435(6)	61(4)
C12	8790(11)	4262(10)	3487(7)	126(7)
C13	7482(8)	2319(9)	2110(8)	99(5)
C14	9434(8)	4240(7)	1394(7)	81(4)
N	11875(6)	1452(5)	−758(5)	52(3)
C15	13130(8)	1395(8)	−582(7)	74(4)
C16	14300(8)	2248(8)	−1059(8)	79(4)
C17	14268(7)	3256(7)	−1767(6)	55(3)
C18	12967(9)	3290(7)	−1946(7)	81(4)
C19	11838(8)	2400(8)	−1440(7)	73(4)
C20	15569(8)	4240(8)	−2258(8)	77(4)
C21	16402(10)	3592(10)	−2840(10)	161(7)
C22	16403(13)	5236(12)	−1349(11)	229(9)
C23	15237(11)	5033(13)	−3204(13)	243(11)

[a]The equivalent isotropic U is defined as one third of the trace of the orthogonalized U_{ij} tensor.

Table 3
Atom coordinates ($\times 10^4$) and equivalent isotropic displacement parameters[a] (Å^2) for Mn(Bupy)$_2$(3,6-DBCat)$_2$

	x/a	y/b	z/c	U_{eq}
Mn	0	0	0	30(2)
O1	381(9)	−1411(8)	−792(8)	40(5)
O2	−1068(10)	−26(9)	−1369(8)	43(5)
N1	−1739(13)	−1353(11)	723(10)	41(6)
C1	−154(14)	−1672(13)	−1921(14)	29(6)
C2	29(17)	−2615(15)	−2791(15)	49(8)
C3	−658(20)	−2815(17)	−3912(14)	66(10)
C4	−1465(19)	−2088(17)	−4223(14)	63(9)
C5	−1610(16)	−1106(15)	−3425(15)	44(8)
C6	−988(15)	−925(14)	−2258(15)	37(7)
C7	−2514(20)	−262(18)	−3767(15)	65(10)
C8	−1612(19)	1267(17)	−3527(14)	77(10)
C9	−3783(19)	−666(20)	−3077(18)	98(11)
C10	−2946(22)	−545(19)	−5138(15)	112(14)
C11	1023(22)	−3332(20)	−2425(15)	70(11)
C12	464(21)	−4237(17)	−1370(14)	94(12)
C13	2490(22)	−2331(21)	−2121(18)	113(15)
C14	1028(22)	−4360(18)	−3496(13)	114(15)
C15	−1710(17)	−2405(15)	1344(13)	49(7)
C16	−2833(18)	−3284(17)	1861(15)	65(9)
C17	−4132(17)	−3221(15)	1749(14)	46(7)
C18	−4170(20)	−2159(16)	1105(14)	66(9)
C19	−2999(19)	−1283(15)	635(14)	59(9)
C20	−5409(22)	−4200(20)	2262(18)	73(10)
C21	−6322(33)	−5260(27)	1387(24)	253(25)
C22	−5144(28)	−5085(28)	3189(27)	250(26)
C23	−6331(27)	−3642(23)	2913(25)	184(19)

[a]The equivalent isotropic U is defined as one third of the trace of the orthogonalized U_{ij} tensor.

DBCat). An initial cycle of refinement was carried out with atom locations obtained from the iron structure determination, subsequent cycles of refinement converged with discrepancy indices of $R=0.078$ and $R_w=0.090$. Selected atom positions are listed in Table 3; see also Section 4.

2.4.3. *Co(Bupy)$_2$(3,6-DBSQ)(3,6-DBCat)*

Dark blue crystals of the complex were obtained from hexane solution. Axial photographs indicated only triclinic symmetry. Unit cell dimensions and the intensities of reflections obtained using Wycoff scans indicated that the complex was isostructural with the iron and manganese analogs. No further refinement was carried out.

3. Results

Synthetic routes to the M(Bupy)$_2$(3,6-DBQ)$_2$ (M = Mn, Fe, Co) series follow procedures that have been used to form related complexes prepared with either other nitrogen coligands or with other quinones [3–5]. Related complexes of cobalt nearly all contain chelating bidentate N-donor ligands [3,6]; Co(Bupy)$_2$-(3,6-DBQ)$_2$ and the [Co(pyz)(3,6-DBQ)$_2$]$_n$ polymer are the only examples with axial structures [7]. Equilibria between valence tautomers occur in separate electron transfer (1) and spin transition (2) steps [3].

$$Co^{III}(N\text{-}N)(DBSQ)(DBCat) \rightleftharpoons Co^{II}*(N\text{-}N)(DBSQ)_2 \quad (1)$$

$$Co^{II}*(N\text{-}N)(DBSQ)_2 \rightleftharpoons Co^{II}(N\text{-}N)(DBSQ)_2 \quad (2)$$

The Cat → Co(III) step occurs at unusually low energy (4000 cm^{-1}) producing a transient low-spin Co(II)* intermediate [3,7]. The metal center of this complex undergoes spin transition in the second step to give the high-spin Co(II) product. Both steps are sensitive to environmental effects [3c,6b] and it has been of interest to see if the shift from a *cis* to *trans* disposition of N-donor coligands effects the tautomeric equilibrium.

Trans-Mn(Bupy)$_2$(3,6-DBQ)$_2$ is closely related to *trans*-Mn(py)$_2$(3,5-DBQ)$_2$ reported earlier [4a]. Spectroscopic changes led to the conclusion that the complex exhibited a tautomeric equilibrium between Mn(IV) and Mn(II) forms in toluene solution (3).

$$Mn^{IV}(py)_2(3,5\text{-}DBCat)_2 \rightleftharpoons Mn^{II}(py)_2(3,5\text{-}DBSQ)_2 \quad (3)$$

More recently, we have been able to provide characterization on all three members of the Mn^{IV}(N-N)(DBCat)$_2$–Mn^{III}(N-N)(DBSQ)(DBCat)–Mn^{II}(N-N)-(DBSQ)$_2$ tautomeric series [4b]. It has been of interest to see if an Mn(III) species appears as an intermediate in the equilibrium involving Mn(II) and Mn(IV) tautomers in the solid state.

With its location between Mn and Co in the first transition series, iron may also show tautomeric equilibria between Fe^{III}(N-N)(DBSQ)(DBCat) and Fe^{II}-(N-N)(DBSQ)$_2$ species. Electron transfer within an Fe^{III}(Cat) complex unit has been implicated in the dioxygen activation step of biological and synthetic catechol oxidation systems [8]. *Trans*-Fe(Bupy)$_2$(3,6-DBSQ)(3,6-DBCat) has been prepared and fully characterized. The results of this investigation are described below.

3.1. *Co(Bupy)$_2$(3,6-DBQ)$_2$*

In contrast with related complexes containing chelating N-donor coligands, Co(Bupy)$_2$(3,6-DBQ)$_2$ is subject to dissociation and decomposition in solution (toluene, hexane) at room temperature in the absence of excess pyridine. Consequently, solution equilibria have not been investigated in detail. Given the kinetic stability of low-spin Co(III) complexes it is likely that the species responsible for decomposition is the Co(II) tautomer, Co^{II}(Bupy)$_2$(3,6-DBSQ)$_2$. Spectra recorded in pyridine/toluene solutions show bands at both 590 and 810 nm that are characteristic of the Co(III) and Co(II) tautomers, respectively. In pyridine the Co(III) tautomer is the sole component. As the toluene composition of the solution is increased the 800 nm band grows in relative intensity and the 590 nm band decreases. In general, the Co(III) tautomer is favored in polar solvents and at low temperatures. Crystals of the complex have been observed to form in the same centrosymmetric triclinic unit cell as found for the Mn and Fe analogs (vide infra) indicating that the pyridine ligands are in a *trans* disposition about the metal. Optical spectra recorded for the complex in the solid state (Fig. 1) show a sharp transition at 600 nm with no band intensity in the 800 nm region. Intense transitions also appear at 1330 and 1700 nm, but the band that dominates the low-energy region of the spectrum appears at 2650 nm. Transitions in the 2500 nm region appear characteristically for the Co^{III}(N-N)(DBSQ)-(DBCat) series and have been assigned as Cat → Co(III) CT transitions [3]. Thermal electron transfer occurs at energies further into the IR, accounting for the thermal accessibility of the Co^{II}(N-N)(DBSQ)$_2$ charge distribution in solution. The structure and spectroscopy of *trans*-Co(Bupy)$_2$(3,6-DBQ)$_2$ are quite similar to the [Co(pyz)(3,6-DBQ)$_2$]$_n$ polymer with the difference that at room temperature both Co(III) and Co(II) tautomers

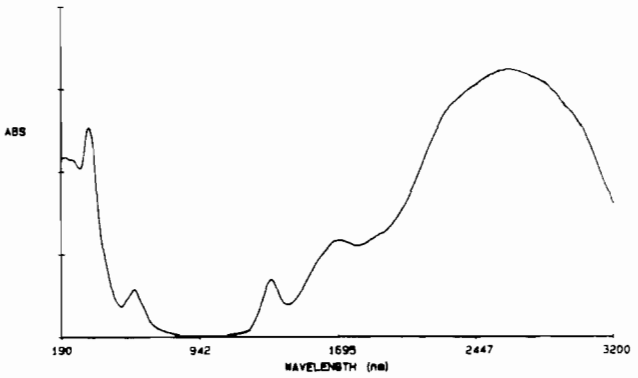

Fig. 1. Electronic spectrum of *trans*-Co^{III}(Bupy)$_2$(3,6-DBSQ)(3,6-DBCat) recorded in the solid state as a KBr pellet.

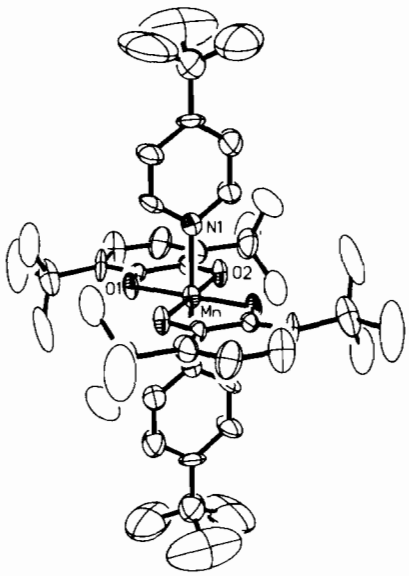

Fig. 2. View of the *trans*-Mn(Bupy)$_2$(3,6-DBQ)$_2$ molecule.

are present in solid samples of the polymer [7]. The Co(III)/Co(II) transition temperature is clearly lower for the polymer, but both complexes with *trans* structures show evidence for tautomeric equilibria.

3.2. *Mn(Bupy)$_2$(3,6-DBQ)$_2$*

Crystallographic characterization on *trans*-Mn(Bupy)$_2$(3,6-DBQ)$_2$ has shown that the molecule has the structure shown in Fig. 2. Bond lengths to the Mn center are often indicative of oxidation state [4]. The d^3 Mn(IV) ion tends to have relatively short Mn–O and Mn–N lengths, the Mn(III) center of *trans*-Mn^{III}(4,4′-bpy)$_2$(3,6-DBSQ)(3,6-DBCat) has short Mn–O lengths but long Mn–N lengths, and Mn^{II}(NO$_2$phen)(3,6-DBSQ)$_2$ has long Mn–O and Mn–N lengths and a trigonal prismatic coordination geometry [4]. Lengths to the metal of *trans*-Mn(Bupy)$_2$(3,6-DBQ)$_2$ are consistent with Mn(IV) in the solid state at room temperature, and the complex is quite similar in structure to *trans*-Mn(py)$_2$(3,5-DBCat)$_2$ (Table 4). Spectro-

Table 4
Selected bond lengths (Å) and angles (°) for *trans*-$Mn^{IV}(Bupy)_2(3,6\text{-}DBCat)_2$, *trans*-$Mn^{IV}(py)_2(3,5\text{-}DBCat)_2$[a], *trans*-$Mn^{III}(4,4'\text{-}bpy)_2(3,6\text{-}DBSQ)(3,6\text{-}DBCat)$[b] and $Mn^{II}(NO_2phen)(3,6\text{-}DBSQ)_2$[b]

	$Mn^{IV}(Bupy)_2(3,6\text{-}DBCat)_2$	$Mn^{IV}(py)_2(3,5\text{-}DBCat)_2$	$Mn^{III}(4,4'\text{-}bpy)_2(3,6\text{-}DBSQ)(3,6\text{-}DBCat)$	$Mn^{II}(NO_2phen)(3,5\text{-}DBSQ)_2$
Mn–O	1.854(10), 1.868(10)	1.853(2), 1.854(2)	1.883(4), 1.889(5)	2.133(5)–2.148(5)
Mn–N	2.034(11)	2.018(3)	2.273(7)	2.283(7), 2.296(6)
C–O	1.333(17), 1.362(19)	1.348(4), 1.349(4)	1.334(7), 1336(8)	1.253(9)–1.282(9)
O–Mn–O	86.7	86.54(9)	85.0(2)	74.6(2), 74.8(3)

[a]Ref. [4a].
[b]Ref. [4b].

scopic characterization on a solid sample at room temperature shows the intense transition at 850 nm that appears for both Mn(IV) and Mn(III) forms of the Mn(N-N)$(DBQ)_2$ complexes (Fig. 3). In the low energy region of the spectrum there is the appearance of a transition at 2120 nm that is characteristic of the Mn(III) charge distribution, $Mn^{III}(Bupy)_2(3,6\text{-}DBSQ)(3,6\text{-}DBCat)$ [4b]. This band increases in intensity reversibly with increasing temperature (Fig. 4). Temperature-dependent changes in the spectrum provide evidence for the Mn(IV)/Mn(III) equilibrium (4) in the solid state with the Mn(III) charge distribution favored at higher temperatures.

$$Mn^{IV}(Bupy)_2(3,6\text{-}DBCat)_2 \rightleftharpoons Mn^{III}(Bupy)_2(3,6\text{-}DBSQ)(3,6\text{-}DBCat) \quad (4)$$

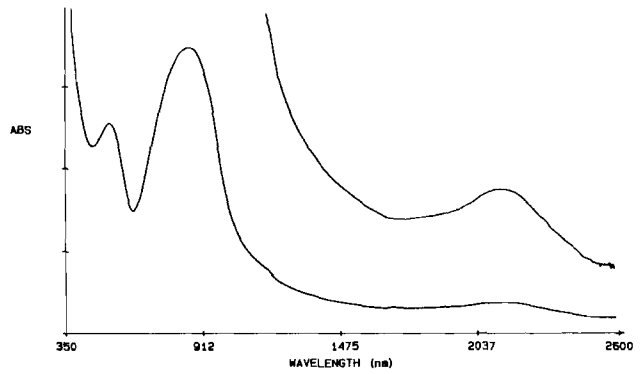

Fig. 3. Electronic spectrum of *trans*-Mn(Bupy)$_2$(3,6-DBQ)$_2$ recorded in the solid state as a KBr pellet.

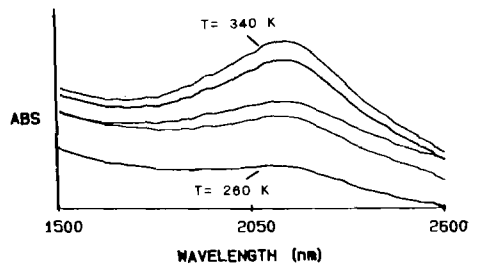

Fig. 4. Temperature dependent changes in the 2100 nm transition of *trans*-$Mn^{III}(Bupy)_2(3,6\text{-}DBSQ)(3,6\text{-}DBCat)$ in the solid state.

In toluene solution at room temperature Mn(Bupy)$_2$(3,6-DBQ)$_2$ appears to decompose by ligand dissociation. This may occur by formation of the $Mn^{II}(Bupy)_2(3,6\text{-}DBSQ)_2$ species as in the case of $Mn(py)_2(3,5\text{-}DBSQ)_2$. With a small quantity of pyridine in the solution the complex is stabilized and the spectral dependence upon composition of a toluene/pyridine solution follows the behavior of the Co analog. The Mn(IV) tautomer is favored at low temperature and high solvent polarity. Shifts in equilibria are accompanied by a dramatic change in color of the solution, from the intense purple color of the Mn(IV) tautomer to a pale green–brown. Bands recorded in a 1:10 pyridine/dichloromethane solution at 300 K appear at 345 (3050 M^{-1} cm^{-1}), 401 (2400), 551 (800), and 823 (1500) nm, and the solution contains an equilibrium mixture of tautomers.

Magnetic measurements have been useful for observing the Co(III)/Co(II) transition of the Co(N-N)$(DBQ)_2$ series [3,6,7] but antiferromagnetic coupling between the radical semiquinone electrons and the dπ metal spins makes such differentiation impossible with Mn [4b]. Complexes of all three charge distributions, $Mn^{IV}(N\text{-}N)(Cat)_2$, $Mn^{III}(N\text{-}N)(SQ)(Cat)$ and $Mn^{II}(N\text{-}N)(SQ)_2$, may have $S = 3/2$ magnetic ground states. The magnetic moment of Mn(Bupy)$_2$(3,6-DBQ)$_2$ drops slowly from the value of 4.25 μ_B at 350 K to 3.8 μ_B at 20 K (Fig. 5). No clear break occurs that might be associated with a sharp Mn(IV)/Mn(III) transition in the solid state.

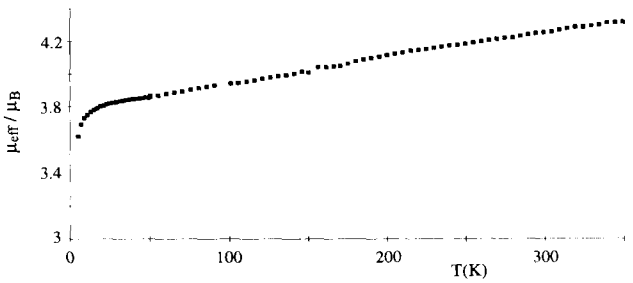

Fig. 5. Plot of magnetic moment (μ_B) vs. temperature (K) for *trans*-Mn(Bupy)$_2$(3,6-DBQ)$_2$.

3.3. Fe(Bupy)$_2$(3,6-DBSQ)(3,6-DBCat)

The Fe(N-N)(DBSQ)(DBCat) complexes prepared with the 3,6-DBBQ ligand have been considerably easier to characterize than related complexes prepared with 3,5-DBBQ [9,10]. Bulky substituents at positions adjacent to both oxygen atoms block bridging interactions that result in the formation of oligomers with 3,5-DBQ. Mössbauer spectroscopy has been used to establish that the metal is high-spin Fe(III) with mixed-charge quinone ligands for various members of the series and similarities in structure, electrochemistry and spectroscopy indicate that Fe(Bupy)$_2$(3,6-DBSQ)(3,6-DBCat) has the same charge distribution [5,9–11]. Electronic spectra on the Fe(N-N)(SQ)(Cat) complexes typically show transitions in three spectral regions, 350–450, 500–600 and 700–900 nm. Bands in all three regions show solvent dependence such that in one solvent medium they appear sharp and intense, in another they split to give a more complicated spectrum. This behavior will be described for the complexes containing chelating N-N ligands in more detail in a separate paper [10]. Spectra obtained for Fe(Bupy)$_2$(3,6-DBSQ)(3,6-DBCat) in a 4:1 toluene/pyridine solution appear similar to spectra of complexes containing chelating ligands. Three bands are observed in solution at 413 (2400 M^{-1} cm^{-1}), 563 (1700) and 835 (2000) nm. In the solid state spectrum (Fig. 6) the two transitions at higher energy appear overlapped to give a band at 538 nm, and the lower energy band appears unchanged in position at 835 nm but with greater relative intensity. At still lower energy in the solid state a transition appears at 2100 nm, the general region where the related complexes of Co(III) and Mn(III) show intense charge transfer bands. This low energy feature also appears for Fe(py)$_2$(3,6-DBSQ)(3,6-DBCat) at 2100 nm, but it is not observed for complexes prepared with chelating N-N ligands [5,9–11]. The nature of these low energy transitions is unclear, but a plausible tentative assignment based on the Co and Mn analogs is as Cat → Fe(III) CT bands that appear uniquely for *trans*-Fe(py)$_2$(3,6-DBSQ)(3,6-DBCat) complexes.

The stability of Fe(Bupy)$_2$(3,6-DBSQ)(3,6-DBCat) has permitted electrochemical characterization in a pyridine/CH_2Cl_2 solution. Redox couples appear at −0.34 and −0.86 V (versus Fc/Fc$^+$) that correspond to oxidation and reduction process associated with the quinone ligands (5), and the Fe(III)/Fe(II) couple appears at −1.42 V.

$$Fe^{III}(Bupy)_2(3,6\text{-}DBSQ)_2^{+} \overset{e^-}{\rightleftharpoons} Fe^{III}(Bupy)_2(3,6\text{-}DBSQ)(3,6\text{-}DBCat)$$

$$Fe^{III}(Bupy)_2(3,6\text{-}DBSQ)(3,6\text{-}DBCat) \overset{e^-}{\rightleftharpoons} Fe^{III}(Bupy)_2(3,6\text{-}DBCat)_2^{-} \quad (5)$$

$$Fe^{III}(Bupy)_2(3,6\text{-}DBCat)_2^{-} \overset{e^-}{\rightleftharpoons} Fe^{II}(Bupy)_2(3,6\text{-}DBCat)_2^{2-}$$

The ligand based couples appear at potentials shifted by nearly 1.0 V negative of the corresponding couples of Fe(bpy)(Cl_4SQ)(Cl_4Cat); the metal reduction step is comparable to the second reduction of the tetrachloroquinone complex [5]. Magnetic measurements on Fe(Bupy)$_2$(3,6-DBSQ)(3,6-DBCat) have shown that the magnetic moment for the complex at 350 K is 5.50 μ_B, with a decrease to values below 4.7 μ_B at 5 K. Strong antiferromagnetic exchange between the radical ligand and the $S=5/2$ metal ion would give a $S=2$ ground state with a moment of 4.90 μ_B. The temperature-dependent behavior shown in Fig. 7 appears to result from thermal population of a higher order spin state at high temperature to give a magnetic moment that is close to that of Fe(bpy)(Cl_4SQ)(Cl_4Cat) (5.50 μ_B). The behavior at low temperature appears to result from weak intermolecular effects.

Difficulties with purity and stability have inhibited the crystallization of Fe(N-N)(SQ)(Cat) complexes, but with the 3,6-DBQ ligand the complexes are quite stable and may be easily crystallized. The structure of *trans*-Fe(Bupy)$_2$(3,6-DBSQ)(3,6-DBCat) is shown in Fig. 8 as the first iron complex of this type to be characterized crystallographically. Bond lengths and angles contained

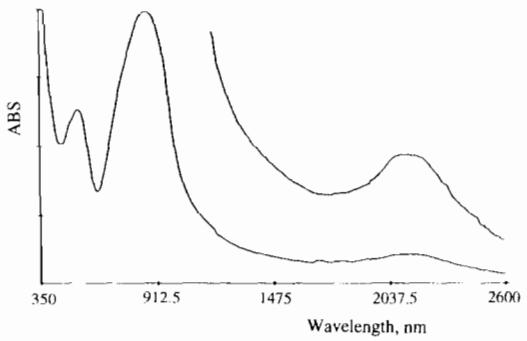

Fig. 6. Electronic spectrum of *trans*-Fe(Bupy)$_2$(3,6-DBSQ)(3,6-DBCat) recorded in the solid state as a KBr pellet.

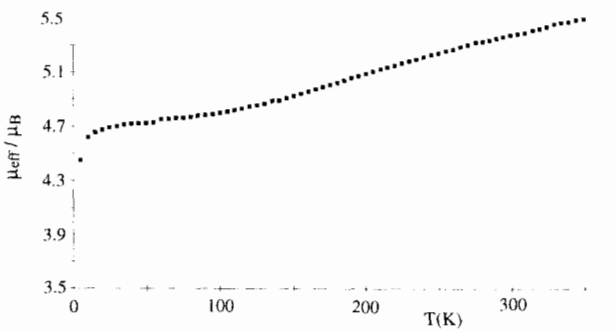

Fig. 7. Plot of magnetic moment (μ_B) vs. temperature (K) for *trans*-Fe(Bupy)$_2$(3,6-DBSQ)(3,6-DBCat).

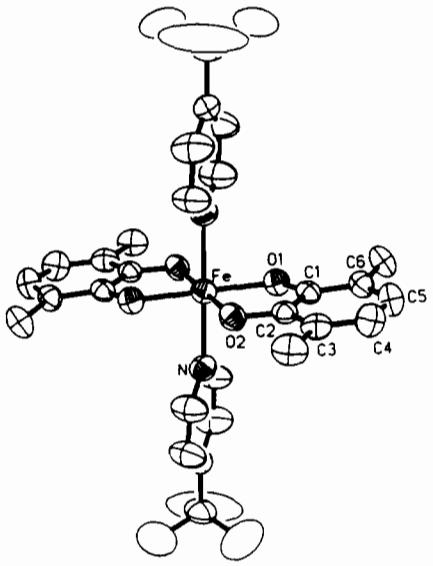

Fig. 8. View of the *trans*-Fe(Bupy)$_2$(3,6-DBSQ)(3,6-DBCat) molecule.

Table 5
Selected bond lengths (Å) and angles (°) for *trans*-Fe(Bupy)$_2$(3,6-DBSQ)(3,6-DBCat)

Fe–O	1.968(4), 1.973(5)
Fe–N	2.205(5)
C–O	1.307(8), 1.315(8)
O–Fe–O	82.0(2)

in Table 5 show values for the Fe–N and Fe–O lengths that are typical of high-spin Fe(III). Structural distinction between the SQ and Cat ligands is lost with the imposed inversion symmetry on the complex molecule. The C–O lengths of 1.307(8) and 1.315(8) are intermediate between values found typically for SQ and Cat ligands, and superposition of ligands of different charge would probably not result in unusual atomic thermal parameters.

3.4. Valence tautomerism for complexes of the M(Bupy)$_2$(3,6-DBQ)$_2$ series

A unique feature of the quinone complexes is their ability to reversibly transfer electrons between ligand and metal under thermal conditions. We have described this behavior for complexes of Co and Mn, and other examples with Ni, Cu, Rh and Ir have appeared [12]. The shift in the center of reactivity within the complex that would accompany the change in charge distribution is a feature of interest, and particularly for the complexes of iron. Electrochemical characterization on catecholate complexes of Fe(III) that include $Fe(Cat)_3^{3-}$, Fe(N-N)(SQ)(Cat) and $FeL_4(Cat)^+$ species, has shown that the Fe(III)/Fe(II) couple appears at a potential that is more negative than −1.0 V [13]. The metal center of an Fe^{II}(Cat) complex would be extremely reductive, and the only examples of complexes of this form are a series of bi- and tetranuclear oligomers reported by Shoner and Power [14].

The Fe(II) species formed as the product of a tautomeric shift in charge distribution, similar to that of the Co and Mn complexes (Eqs. (1)–(3)), would contain and $Fe^{II}(SQ)_2$ species (6).

$$Fe^{III}(N\text{-}N)(SQ)(Cat) \rightleftharpoons Fe^{II}(N\text{-}N)(SQ)_2 \quad (6)$$

No complex of this charge distribution has been isolated, but low-spin Fe(Cp)(CO)(3,5-DBSQ) has been reported [15] and the Fe(II) center of an Fe^{II}(SQ) species may be less nucleophilic than the corresponding Cat complex due to differences in Cat and SQ oxygen donation. In contrast to the temperature dependence observed for Co(Bupy)$_2$(3,6-DBQ)$_2$ and Mn(Bupy)$_2$(3,6-DBQ)$_2$, spectra obtained for Fe(Bupy)$_2$(3,6-DBSQ)(3,6-DBCat) show no temperature dependence. Further, there is no behavior in the solid state or in solution to suggest that complexes of the iron series undergo tautomeric transitions of the type described in Eq. (6), and it becomes important to understand the difference between this reaction and the Co and Mn equilibria. Changes in magnetic spin degeneracy are thought to provide a positive entropy change that favors the transition to high-spin $Co^{II}(SQ)_2$ and $Mn^{II}(SQ)_2$ species at temperatures defined by the ratio of collective enthalpic and entropic changes associated with the steps in the equilibrium [3c,4b]. The change in spin degeneracy would be smaller for the Fe^{III}(Cat)/Fe^{II}(SQ) transition, and the thermodynamic potential associated with the thermal shift in charge distribution is lost in the case of iron. Assuming that Cat → M electron transfer occurs at thermally accessible energies for all three metal ions on the basis of low energy transitions, the resulting Fe^{II}(Bupy)$_2$(3,6-DBSQ)$_2$ product would be thermodynamically unstable and short-lived, while with Co and Mn, at a favorable temperature, electron transfer provides an entry to the tautomeric equilibria.

Two fundamental conditions appear to be important for valence tautomeric equilibria. Ligand field effects must be such that metal–quinone electron transfer occurs with facility. There are many examples of Co^{III}(Cat) coordination that fail to show electron transfer properties [16]. Secondly, entropic changes are necessary for temperature-dependent shifts in component concentration. Changes in spin degeneracy, of the type associated with spin transition equilibria [17], are responsible for shifts in equilibria for the Co(N-N)(DBQ)$_2$ and Mn(N-N)(DBQ)$_2$ series, while for the Fe(N-N)(DBQ)$_2$ no temperature dependence is observed, even for cases where the conditions for Cat → Fe(III) electron transfer are favorable.

4. Supplementary material

Tables containing a full listing of atom positions, bond lengths and angles, anisotropic displacement parameters and hydrogen atom locations are available for $Fe(Bupy)_2(3,6\text{-}DBSQ)(3,6\text{-}DBCat)$ and $Mn(Bupy)_2(3,6\text{-}DBCat)_2$.

Acknowledgement

We would like to thank Brenda Conklin for magnetic susceptibility measurements. Support for this research was provided by the National Science Foundation through Grant CHE 90-23636.

References

[1] C.G. Pierpont and C.W. Lange, *Prog. Inorg. Chem., 41* (1994) 331.
[2] (a) I.S. Belostotskaya, N.L. Komissarova, E.V. Dzhuaryan and V.V. Ershov, *Izv. Akad. Nauk, SSSR,* (1972) 1594; (b) A.S. Attia and C.G. Pierpont, submitted for publication.
[3] (a) R.M. Buchanan and C.G. Pierpont, *J. Am. Chem. Soc., 102* (1980) 4951; (b) O.-S. Jung and C.G. Pierpont, *J. Am. Chem. Soc., 116* (1994) 1127; (c) *Inorg. Chem., 33* (1994) 2227.
[4] (a) M.W. Lynch, D.N. Hendrickson, B.J. Fitzgerald and C.G. Pierpont, *J. Am. Chem. Soc., 106* (1984) 2041; (b) A.S. Attia and C.G. Pierpont, submitted for publication.
[5] D. Zirong, S. Bhattacharya, J.K. McCusker, P.M. Hagen, D.N. Hendrickson and C.G. Pierpont, *Inorg. Chem., 31* (1992) 870.
[6] (a) G.A. Abakumov, V.K. Cherkasov, M.P. Bubnov, O.G. Ellert, Z.B. Dobrokhotova, L.N. Zakharov and Y.T. Struchkov, *Dokl. Akad. Nauk, 328* (1993) 12; (b) D.M. Adams, A. Dei, A.L. Rheingold and D.N. Hendrickson, *J. Am. Chem. Soc., 115* (1993) 8221.
[7] O.-S. Jung and C.G. Pierpont, *J. Am. Chem. Soc., 116* (1994) 2229.
[8] (a) H.G. Jang, D.D. Cox and L. Que, Jr., *J. Am. Chem. Soc., 113* (1991) 9200; (b) T. Funabiki, H. Kojima, M. Kaneko, T. Inoue, T. Yoshioka, T. Tanaka and S. Yoshida, *Chem. Lett.* (1991) 2143.
[9] M.W. Lynch, M. Valentine and D.N. Hendrickson, *J. Am. Chem. Soc., 104* (1982) 6982.
[10] A.S. Attia and C.G. Pierpont, submitted for publication.
[11] M.J. Cohn, C.-L. Xie, J.-P.M. Tuchagues, C.G. Pierpont and D.N. Hendrickson, *Inorg. Chem., 31* (1992) 5028.
[12] (a) G.A. Abakumov, G.A. Razuvaev, V.I. Nevodchikov and V.K. Cherkasov, *J. Organomet. Chem., 341* (1988) 485; (b) R.R. Rakhimov, P.M. Solozhenkin, N.N. Kopitaya, V.S. Pupkov and A.I. Prokof'ev, *Dokl. Akad. Nauk SSSR, 300* (1988) 1177; (c) G.A. Abakumov, V.A. Garnov, V.I. Nevodchikov and V.K. Cherkasov, *Dokl. Akad. Nauk SSSR, 304* (1989) 107.
[13] (a) S.J. Rodgers, C.-W. Lee, C.Y. Ng and K.N. Raymond, *Inorg. Chem., 26* (1987) 1622; (b) D.D. Cox and L. Que, Jr., *J. Am. Chem. Soc., 110* (1988) 8085.
[14] S.C. Shoner and P.P. Power, *Inorg. Chem., 31* (1992) 1001.
[15] K. Sarbasov, S.P. Solodovnikov, B.L. Tumanskii, N.N. Bubnov and A.I. Prokof'ev, *Izv. Akad. Nauk, SSSR, Ser. Khim.,* (1982) 1509.
[16] (a) P.A. Wicklund and D.G. Brown, *Inorg. Chem., 15* (1976) 396; (b) S.L. Kessel, R.M. Emberson, P.G. DeBrunner and D.N. Hendrickson, *Inorg. Chem., 19* (1980) 1170; (c) F. Hartl and A. Vlcek, Jr., *Inorg. Chim. Acta, 118* (1986) 57; (d) C. Bianchini, D. Masi, C. Mealli, A. Meli, G. Martini, F. Laschi and P. Zanello, *Inorg. Chem., 26* (1987) 3683; (e) C. Benelli, A. Dei, D. Gatteschi and L. Pardi, *Inorg. Chim. Acta, 163* (1989) 99.
[17] (a) P. Gutlich, *Struct. Bonding (Berlin), 44* (1981) 83; (b) E. Konig, *Prog. Inorg. Chem., 35* (1987) 527.